



EXPERIMENTAL ENERGY LEVELS AND PARTITION FUNCTION OF THE $^{12}\text{C}_2$ MOLECULE

TIBOR FURTENBACHER¹, ISTVÁN SZABÓ¹, ATTILA G. CSÁSZÁR¹, PETER F. BERNATH², SERGEI N. YURCHENKO³, AND
JONATHAN TENNYSON³

¹ Institute of Chemistry, Eötvös Loránd University and MTA-ELTE Complex Chemical Systems Research Group,
H-1518 Budapest 112, P.O. Box 32, Hungary; csaszar@chem.elte.hu

² Department of Chemistry, Old Dominion University, Norfolk, VA, USA

³ Department of Physics and Astronomy, University College London, London WC1E 6BT, UK; j.tennyson@ucl.ac.uk

Received 2016 February 22; revised 2016 April 26; accepted 2016 April 26; published 2016 June 24

ABSTRACT

The carbon dimer, the $^{12}\text{C}_2$ molecule, is ubiquitous in astronomical environments. Experimental-quality rovibronic energy levels are reported for $^{12}\text{C}_2$, based on rovibronic transitions measured for and among its singlet, triplet, and quintet electronic states, reported in 42 publications. The determination utilizes the Measured Active Rotational-Vibrational Energy Levels (MARVEL) technique. The 23,343 transitions measured experimentally and validated within this study determine 5699 rovibronic energy levels, 1325, 4309, and 65 levels for the singlet, triplet, and quintet states investigated, respectively. The MARVEL analysis provides rovibronic energies for six singlet, six triplet, and two quintet electronic states. For example, the lowest measurable energy level of the a $^3\Pi_u$ state, corresponding to the $J = 2$ total angular momentum quantum number and the F_1 spin-multiplet component, is $603.817(5)\text{cm}^{-1}$. This well-determined energy difference should facilitate observations of singlet–triplet intercombination lines, which are thought to occur in the interstellar medium and comets. The large number of highly accurate and clearly labeled transitions that can be derived by combining MARVEL energy levels with computed temperature-dependent intensities should help a number of astrophysical observations as well as corresponding laboratory measurements. The experimental rovibronic energy levels, augmented, where needed, with ab initio variational ones based on empirically adjusted and spin–orbit coupled potential energy curves obtained using the DUO code, are used to obtain a highly accurate partition function, and related thermodynamic data, for $^{12}\text{C}_2$ up to 4000 K.

Key words: molecular data

Supporting material: FITS file, machine-readable table

1. INTRODUCTION

The rovibronic spectra of $^{12}\text{C}_2$, involving singlet, triplet, and quintet electronic states, are rich and complex in features as well as in anomalies. This is true despite the fact that $^{12}\text{C}_2$, hereafter simply called C_2 , is a homonuclear diatomic molecule containing only eight valence electrons. There are 62 electronic states corresponding to the 6 possible separated-atom limits formed by different pairs of the $\text{C}(^3\text{P})$, $\text{C}(^1\text{D})$, and $\text{C}(^1\text{S})$ atoms. Eighteen of these states, six singlet, six triplet, and six quintet ones, correspond to the $\text{C}(^3\text{P}) + \text{C}(^3\text{P})$ asymptote. As summarized in Table 1 and Figure 1, the measured rovibronic spectroscopy of C_2 is characterized by 19 known band systems, and a further three intercombination transitions, which cover the spectral range 0–55,000 cm^{-1} and now all three spin states. Due to the lack of detailed transition data (see Section 2.4 for details), only 14 band systems are considered in the present study. All the states considered, except the e $^3\Pi_g$ and the 4 $^3\Pi_g$ states, share the same $\text{C}(^3\text{P}) + \text{C}(^3\text{P})$ separated-atom limit. The present study was initiated as, rather unusually, at least six of these bands have been used for astronomical observations, with another one having been proposed for such use.

There are numerous astronomical observations of C_2 spectra with a multitude of important applications for astrophysics. C_2 spectra have been observed in comets (Mayer & O’Dell 1968), in high-temperature stars (Vartya 1970), translucent clouds (Sonnentrucker et al. 2007), and in the low-temperature interstellar medium (Souza & Lutz 1977). High-quality studies of rotational and spatial distributions of C_2 in comets are available (Lambert 1978; Lambert et al. 1990). The

astronomical observations and their modeling are supported by a number of laboratory studies (Wodtke & Lee 1985; Urdahl et al. 1988; Bao et al. 1991; Jackson et al. 1991; Blunt et al. 1995, 1996). To make maximum use of the observations one needs accurate rovibronic energy level information, the principal topic of the present paper.

Both the Swan (Swings 1943; Gredel et al. 1989; Lambert et al. 1990; Rousselot et al. 2000) and the Deslandres–d’Azambuja (Gredel et al. 1989) bands have been observed in fluorescence from comets. Indeed, two singlet, X $^1\Sigma_g^+$ and A $^1\Pi_u$, and four triplet, a $^3\Pi_u$, b $^3\Sigma_g^+$, c $^3\Sigma_u^+$, and d $^3\Pi_g$, electronic states are needed to model C_2 emission observed in comets. Two spin-forbidden transition systems, a $^3\Pi_u \rightarrow \text{X } ^1\Sigma_g^+$ and c $^3\Sigma_u^+ \rightarrow \text{X } ^1\Sigma_g^+$, are needed to explain the observed intensities in the Swan band (Rousselot et al. 2000).

The astronomical observations include solar spectra, where C_2 forms an important component of the photospheric carbon abundance (Asplund et al. 2005). So, for example, C_2 can be observed in the Sun’s photosphere at visible wavelengths using the Swan band (Asplund et al. 2005) and in the infrared via the Phillips and Ballik–Ramsay bands (Brault et al. 1982). Transitions in the Swan band have also been observed in peculiar white dwarfs (Hall & Maxwell 2008; Kowalski 2010) and the coronae borealis star V coronae australis (Rao & Lambert 2008), while the Phillips band is prominent, for example, in the carbon star HD19557 (Goebel et al. 1983). Transitions in the Ballik–Ramsay band have also been observed in carbon stars (Goorvitch 1990).

Table 1

Singlet, Triplet, and Quintet Band Systems of $^{12}\text{C}_2$ for which Rovibronic Transitions Have Been Reported in the Literature. Band Systems Printed in Italics, due to Reasons Given Below, Are Not Considered in This Paper

Multiplicity	Band System	Transition	Original Detection	
Singlet	Phillips	A $^1\Pi_u-X\ ^1\Sigma_g^+$	Phillips (1948a)	
	Mulliken	D $^1\Sigma_u^+-X\ ^1\Sigma_g^+$	Landsverk (1939)	
	<i>Herzberg F</i>	F $^1\Pi_u-X\ ^1\Sigma_g^+$	Herzberg et al. (1969)	
	Bernath B	B $^1\Delta_g-A\ ^1\Pi_u$	Douay et al. (1988b)	
	Bernath B'	B' $^1\Sigma_g^+-A\ ^1\Pi_u$	Douay et al. (1988b)	
	<i>Deslandres-d'Azambuja</i>	C $^1\Pi_g-A\ ^1\Pi_u$	Deslandres & d'Azambuja (1905)	
	<i>Messlerle-Krauss</i>	C' $^1\Pi_g-A\ ^1\Pi_u$	Messlerle & Krauss (1967)	
	Freymark	E $^1\Sigma_g^+-A\ ^1\Pi_u$	Freymark (1951)	
	<i>Goodwin-Cool A</i>	1 $^1\Delta_u-A\ ^1\Pi_u$	Goodwin & Cool (1988a)	
	<i>Goodwin-Cool B</i>	1 $^1\Delta_u-B\ ^1\Delta_g$	Goodwin & Cool (1988a)	
	Triplet	Ballik-Ramsay	b $^3\Sigma_g^- - a\ ^3\Pi_u$	Ballik & Ramsay (1958)
		Swan	d $^3\Pi_g - a\ ^3\Pi_u$	Swan (1857)
Fox-Herzberg		e $^3\Pi_g - a\ ^3\Pi_u$	Fox & Herzberg (1937)	
<i>Herzberg f</i>		f $^3\Sigma_g^- - a\ ^3\Pi_u$	Herzberg et al. (1969)	
<i>Herzberg g</i>		g $^3\Delta_g - a\ ^3\Pi_u$	Herzberg et al. (1969)	
Krechivska-Schmidt		4 $^3\Pi_g - a\ ^3\Pi_u$	Krechivska et al. (2015)	
Duck		d $^3\Pi_g - c\ ^3\Sigma_u^+$	Kokkin et al. (2006)	
<i>Kable-Schmidt</i>		e $^3\Pi_g - c\ ^3\Sigma_u^+$	Nakajima et al. (2009)	
Quintet		Radi-Bornhauser	1 $^5\Pi_u - 1\ ^5\Pi_g$	Bornhauser et al. (2011)
		Intercombination	triplet-singlet	a $^3\Pi_u - X\ ^1\Sigma_g^+$
quintet-triplet	1 $^5\Pi_g - a\ ^3\Pi_u$		Bornhauser et al. (2011)	
singlet-triplet	A $^1\Pi_u - b\ ^3\Sigma_g^-$		Chen et al. (2015)	

Interstellar C_2 has been observed via the infrared Phillips band, for example, in the Perseus molecular complex (Hobbs 1979; Lambert et al. 1995; Iglesias-Groth 2011) and toward the Cyg OB2 association (Gredel et al. 2001). Emission features from the Swan band have been observed in the Red Rectangle (Wehres et al. 2010). Sonnentrucker et al. (2007) observed absorption in the Phillips, Mulliken and Herzberg F bands in their study of translucent clouds by the simultaneous use of observations from both space and ground-based telescopes.

The rovibrational manifolds of the $X\ ^1\Sigma_g^+$ and $a\ ^3\Pi_u$ states strongly overlap, as the corresponding electronic excitation energy is less than half of the vibrational spacing in either state. Lebourlot & Roueff (1986) suggested that long-wavelength transitions between levels in the $a\ ^3\Pi_u - X\ ^1\Sigma_g^+$ band should provide a good method for monitoring interstellar C_2 . Rousselot et al. (1998) attempted to observe such lines in the Hale-Bopp comet, without success. The accurate rovibronic energy levels presented in this paper can be used to provide accurate transitions for such features.

As for the other bands, at ultraviolet wavelengths the *International Ultraviolet Explorer* was used to observe C_2 toward X Persei via the Herzberg F band (Lien 1984). The *Hubble Space Telescope* also has been used to monitor C_2 absorption in the ultraviolet using both the Mulliken and the Herzberg F bands (Lambert et al. 1995; Hupe et al. 2012).

Finally, we note that all of the bands mentioned are important in laboratory plasmas (Chen & Mazumder 1990; Duxbury et al. 1998; Hornkohl et al. 2011) and flames (Bleekrode & Nieuwpoort 1965; Amiot et al. 1979; Brockhinke et al. 1998; Lloyd & Ewart 1999; Smith et al. 2005; Goldman & Cheskis 2008). For example, there are particular vibrational bands of the Swan system known as the High Pressure (HP)

bands (Herzberg 1946; Little & Browne 1987; Caubet & Dorthe 1994) that can be prominent in such environments at atmospheric pressure.

Studies of the spectra, and thus the band systems, of C_2 date all the way back to Wollaston (1802) and the dawn of spectroscopy, when C_2 emissions were first observed in flames. Detailed studies by Swan (1857) of the most prominent band of C_2 also predate the development of the quantum mechanical tools required to interpret the spectroscopic results obtained. Over the following century and a half, a number of other bands have been detected and studied. Indeed, four band systems have been identified during the last decade (Kokkin et al. 2006; Nakajima et al. 2009; Bornhauser et al. 2011; Krechivska et al. 2015). Table 1 lists the known band systems of C_2 relevant for the present study.

A large number of spectroscopic measurements exist for the different band systems of C_2 . All the studies that contain primary measured transitions at a reasonable level of accuracy are considered during the present analysis. The experimental papers found and analyzed by us are listed here based on the band systems: Phillips (Phillips 1948a; Ballik & Ramsay 1963b; Chauville et al. 1977; Erman et al. 1982; Davis et al. 1988a, 1988c; Douay et al. 1988a; Chan et al. 2004; Petrova & Sinitisa 2006; Nakajima & Endo 2013; Chen et al. 2015), Mulliken (Landsverk 1939; Mulliken 1939), Bernath B (Douay et al. 1988b; Bao et al. 1991), Bernath B' (Douay et al. 1988b), Freymark (Freymark 1951; Blunt et al. 1996), Ballik-Ramsay (Ballik & Ramsay 1963a; Veseth 1975; Amiot et al. 1979; Roux et al. 1985; Yan et al. 1985; Davis et al. 1988b; Petrova & Sinitisa 2006; Bornhauser et al. 2011; Chen et al. 2015), Swan (Swan 1857; Raffety 1916; Callomon & Gilby 1963; Meinel & Messlerle 1968; Phillips 1968; Phillips & Davis 1968; Brewer &

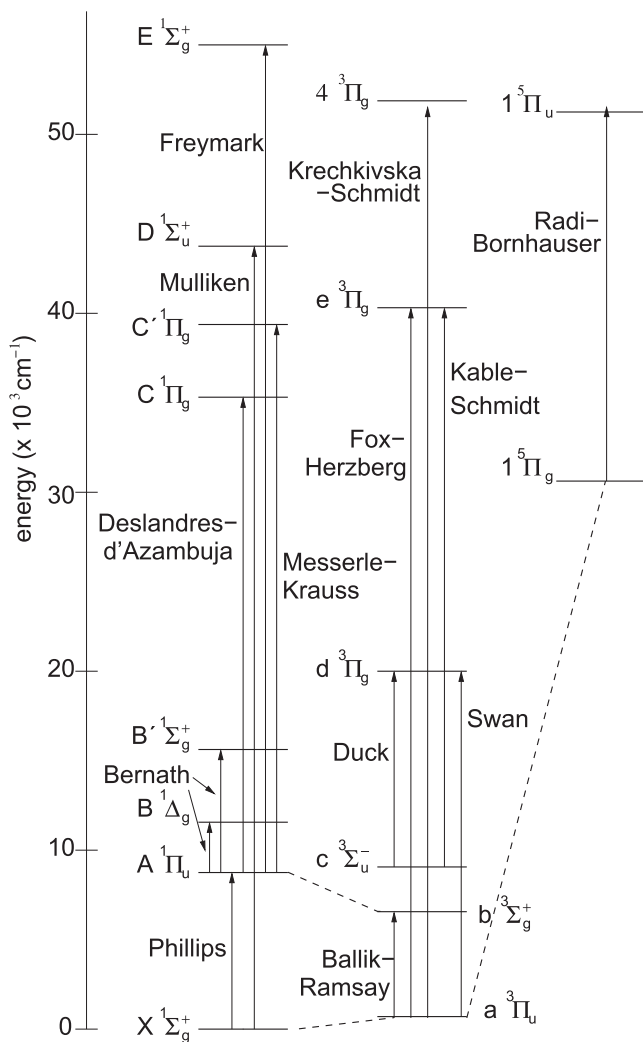


Figure 1. The band system of $^{12}\text{C}_2$ showing the bands considered in this work. The dashed lines represent observed but unnamed intercombination bands.

Hagan 1979; Amiot 1983; Curtis & Sarre 1985; Suzuki et al. 1985; Urdahl et al. 1988; Chen & Mazumder 1990; Kaminski et al. 1997; Lloyd & Ewart 1999; Smith et al. 2005; Kokkin et al. 2006), Fox–Herzberg (Fox & Herzberg 1937), Deslandres–d’Azambuja (Deslandres & d’Azambuja 1905; Antić-Jovanović et al. 1985; van de Burgt & Heaven 1987; Urdahl et al. 1988), Messerle–Krauss (Messerle & Krauss 1967), Goodwin–Cool (Goodwin & Cool 1988a, 1988b, 1989), Duck (van de Burgt & Heaven 1987; Kokkin et al. 2006), Krechkivska–Schmidt (Krechkivska et al. 2015, 2016) and Radi–Bornhauser (Bornhauser et al. 2015), as well as various spin-changing intercombination bands (Bornhauser et al. 2011; Chen et al. 2015).

It is interesting to note that for a long time a triplet state, now named a $^3\Pi_u$, was believed to be the lowest electronic state of C_2 and not a singlet state, the true ground electronic state, $X\ ^1\Sigma_g^+$. The source of the confusion, detailed in Ballik & Ramsay (1959), is that the energy difference between the two electronic states is only about one half of the vibrational fundamental of either state so that the Swan system can be seen in absorption in many sources. The spectroscopy and the spectroscopic constants of C_2 have been the subject of several reviews (Huber & Herzberg 1979; Weltner & Van Zee 1989;

Martin 1992; Van Orden & Saykally 1998). Huber & Herzberg (1979) reported the analysis of seven singlet and seven triplet states. Weltner & Van Zee (1989) reviewed the then available experimental and theoretical results. The spectroscopic and kinetic properties of C_2 , including 23 electronic states studied prior to 1992, were reviewed by Martin (1992). Van Orden & Saykally (1998) reviewed the spectroscopy of small carbon clusters which, once again, covered the extensive spectroscopic literature available for C_2 . The present paper surveys all rovibronically resolved measurements made up to the end of 2015.

A large number of ab initio computations have been performed on C_2 (Kirby & Liu 1979; Bauschlicher & Langhoff 1987; Watts & Bartlett 1992; Boggio-Pasqua et al. 2000; Bruna & Grein 2001; Müller et al. 2001; Abrams & Sherrill 2004; Sherrill & Piecuch 2005a; Kokkin et al. 2007; Booth et al. 2011; Jiang & Wilson 2011; Schmidt & Bacskay 2011; Angeli et al. 2012; Boschen et al. 2013, 2014; Krechkivska et al. 2015, 2016). Notable among the sophisticated electronic structure computations are those of Bacskay (Kokkin et al. 2007; Schmidt & Bacskay 2011; Krechkivska et al. 2015, 2016); for example, they led to the observation of the Duck band and enabled the identification of the Krechkivska–Schmidt band system. Boschen et al. (2013) pointed out that “at the present state of the art, theoretical potential energy curves (PECs) that reproduce the rotational-vibrational levels to spectroscopic accuracy (1 cm^{-1}) or near spectroscopic accuracy (10 cm^{-1}) are considered highly accurate.” Reproduction of measured electronic excitation energies of C_2 appears to be even more problematic; an accuracy of a few hundred cm^{-1} seems to be the norm. Thus, it is still of interest to perform accurate quantum chemical computations on C_2 and its rovibronic states. Results of a preliminary, first-principles analysis are reported here (vide infra), used in particular for checking the experimental transitions and energy levels.

The main body of the present work is a Measured Active Rotational-Vibrational Energy Levels (MARVEL; Furtenbacher et al. 2007; Furtenbacher & Császár 2012a) analysis of the measured rovibronic states of C_2 . Our analysis has been in progress for 4 years but a real breakthrough came with the study of Chen et al. (2015), who observed 16 forbidden transitions between singlet and triplet states. This study coupled, for the first time, the singlet and triplet components of the observed spectroscopic network (SN) (Császár & Furtenbacher 2011; Furtenbacher & Császár 2012b; Császár et al. 2016) of C_2 , allowing a much improved analysis of its rovibronic energy level structure. We analyze all the known bands of C_2 with the exception of the five VUV bands due to Herzberg et al. (1969) and Goodwin & Cool (1988a, 1988b, 1989). These bands involve upper energy levels that arise from a single experiment and are too high for us to be able to independently validate them.

Finally, when a complete set of accurate energy levels is available for a molecule, it can be used, via the direct summation technique, to compute accurate ideal-gas thermodynamic functions, most importantly the high-temperature internal partition function, $Q_{\text{int}}(T)$. We do this here for C_2 , complementing and improving several previous efforts (Altman 1960; Clementi 1961; Irwin 1981; Sauval & Tatum 1984; Rossi et al. 1985; Gurvich & Veyts 1990), and arrive at very precise and accurate values for $Q_{\text{int}}(T)$ of C_2 up to 4000 K.

2. METHODOLOGICAL DETAILS

2.1. Experimental Spectroscopic Network of C_2

The MARVEL (Furtenbacher et al. 2007; Furtenbacher & Császár 2012a) procedure and code is used in this study to obtain rovibronic energies of C_2 by inverting all assigned experimental rovibronic transitions available in the literature for this molecule. MARVEL is based on the concept of SNs (Császár & Furtenbacher 2011; Furtenbacher & Császár 2012b; Császár et al. 2016): SNs are large, finite, weighted, rooted graphs, where the vertices are discrete energy levels (with associated uncertainties), the edges are transitions (with measured uncertainties), and in a simple picture the weights are provided by the transition intensities. No weights are considered during the present study. Within the experimental SN of a molecule there can be several rooted components and several floating ones. For many molecules the rooted components belong to ortho and para nuclear spin isomers. However, the nuclear spin of ^{12}C is zero; thus, $^{12}C_2$ has only one nuclear spin isomer and one root for its lowest electronic state, $X^1\Sigma_g^+$.

Transitions between electronic states of different spin multiplicity are spin forbidden; thus, until 2011 no lines were measured and assigned experimentally between the singlet and triplet and the triplet and quintet manifold of states of C_2 . First, Bornhauser et al. (2011) observed transitions linking triplet and quintet electronic states, leading to the first observation and characterization of a quintet band of C_2 . Later, Chen et al. (2015) managed to identify 16 spin-forbidden transitions between singlet and triplet states. These spin-forbidden transitions proved to be particularly important during the MARVEL analysis of the experimental spectra of C_2 . Using these forbidden transitions the experimental SN of C_2 simplifies because now it contains only one principal component (PC). The label of the root of the PC is $\{0 + X^1\Sigma_g^+ 0 F_1 e\}$, for the notation employed for the label see Section 2.3.

The measured SN of C_2 is shown pictorially in Figure 2; the singlet, triplet, and quintet energy levels are indicated with different colors. Since Figure 2 is a particular representation of a network (i.e., a graph), the arrangement of the nodes (energy levels) and links (transitions) is arbitrary, but clearly displays several important characteristics of the SN of C_2 . Figure 2 vividly shows, for example, how weakly the singlet rovibrational energy levels are connected to the triplet core.

2.2. MARVEL

During a MARVEL analysis we simultaneously process all the available assigned and labeled experimental transitions. The energy levels are obtained from the set of transitions via a weighted linear least-squares inversion protocol. As the MARVEL technique has been employed to determine experimental-quality energy levels of nine isotopologues of water (Tennyson et al. 2009, 2010, 2013, 2014a, 2014b), of three isotopologues of H_3^+ (Furtenbacher et al. 2013a, 2013b), as well as of ammonia (Al Derzi et al. 2015) and ketene (Fábri et al. 2011), the interested reader is referred to these publications for details about the different stages of a MARVEL analysis.

Since C_2 has both regular and inverted triplet states (see the next subsection for details), for example, the $a^3\Pi_u$ and $d^3\Pi_g$ of C_2 are inverted, during the MARVEL analysis it was

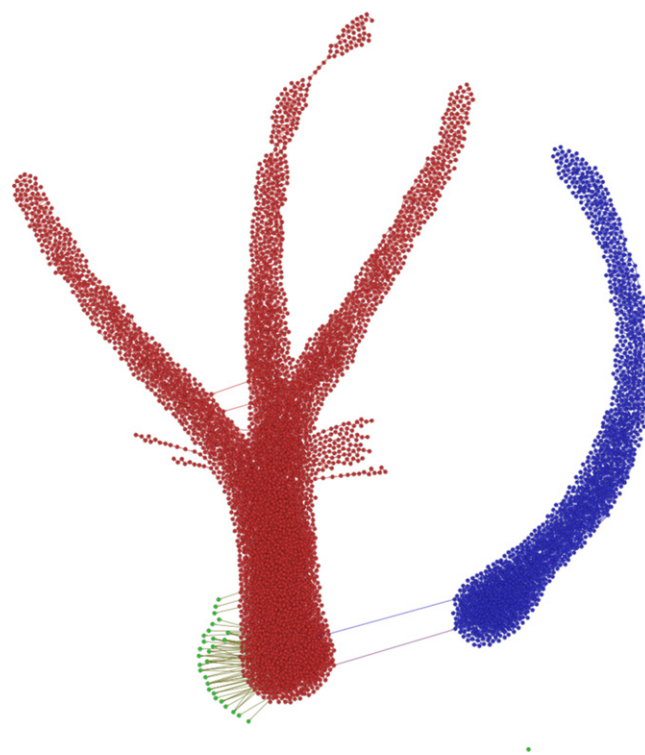


Figure 2. Representation of the experimental spectroscopic network built in this study for $^{12}C_2$. The blue, red, and green dots correspond to the singlet, triplet, and quintet rovibronic states, respectively. The dots represent energy levels and only some of the transitions are visible, especially those connecting the singlet and the triplet as well as the triplet and the quintet rovibrational states.

checked whether the labels of all experimental transitions follow the same convention.

At the beginning, the MARVEL analysis of the spectra of C_2 was complicated by the fact that there have been no truly high-accuracy variational or effective Hamiltonian rovibronic energy levels available for this molecule at higher energies. This situation greatly improved by the first-principles DUO (Yurchenko et al. 2016a) analysis performed as part of this study (vide infra), allowing at least a preliminary validation of the MARVEL levels up to $35,000\text{ cm}^{-1}$.

2.3. Labels and Quantum Numbers

For MARVEL to work properly one needs appropriate and unique labels. The label used in the present study for a rovibronic energy level is built up from information concerning the uncoupled electronic state, the vibrational and rotational quantum numbers, and the symmetry of the rovibronic state.

The label finally chosen for each energy level, $\{J, +/-, \text{state}, \nu, F_i, e/f\}$, fully characterizes the rovibronic states of a homonuclear diatomic molecule, such as C_2 , but contains redundant information (Brown & Carrington 2003; Lefebvre-Brion & Field 2004; Bernath 2016). Here $J \geq 0$ is the quantum number corresponding to the total angular momentum (an integer value) characterizing the state, $+/-$ labels the total state parity, $+1/-1$, in terms of the laboratory-fixed inversion operator E^* (Bernath 2016), “state” is the customary term symbol of the electronic state before spin-orbit coupling is taken into account (e.g., $X^1\Sigma_g^+$ and $b^3\Sigma_g^-$), and ν is the vibrational quantum number. The F_i , $i = 1, 2, \dots, 2S + 1$, label denotes the spin multiplet components: for singlet states $i = 1$,

i.e., $F_i \equiv F_1$, for triplet states $i = 1, 2, 3$, which corresponds to the standard spectroscopic notation F_1, F_2 , and F_3 (F_1, F_2, F_3 refer to levels with $J = N + 1, N, N - 1$, where N is the quantum number corresponding to the angular momentum exclusive of nuclear and electron spin and it is usually not a good quantum number), and for quintet states $i = 1, 2, 3, 4, 5$ (Whiting 1973). The convention (Bernath 2016) is such that whether the state is regular ($A > 0$) or inverted ($A < 0$), the energy order is always $F_3 > F_2 > F_1$ for the triplet states. The g and u subscript in the “state” label indicate if the symmetry of the electronic state is “gerade” (positive) or “ungerade” (negative) in terms of the molecule-fixed inversion operator, i (Bernath 2016). The $+/-$ superscripts within the $\Sigma^{+/-}$ states indicate the parity of the electronic component with respect to vertical reflection, σ_v , in the molecular frame (Bernath 2016). The rotationless parity e/f is a widely used alternative to the total parity $+/-$, this redundant information is included in our MARVEL label to help experimentalists. For C_2 the allowed combination of the parity $+/-$ and the label g/u is $(+, g)$ and $(-, u)$. The rotationless parity e/f is then obtained as follows: (a) for the e states, the parity $(+1$ or $-1)$ can be recovered as $(-1)^J$, i.e., for the even values of J the parity of the e states is $+1$, while for odd J s it is -1 ; and (b) for the f states, the parity is recovered as $(-1)^{J+1}$, i.e., for even J s the parity is -1 , and for odd J s it is $+1$.

The rigorous electric dipole selection rules for the rovibronic transitions are

$$J'' - J' = \pm 1, 0, \quad , \quad 0 \not\leftrightarrow 0, \quad (1)$$

$$+ \leftrightarrow - \quad , \quad g \leftrightarrow u. \quad (2)$$

As mentioned, the nuclear spin statistical weight g_{ns} of the nuclear spin-zero $^{12}C_2$ molecule for the $(+, g)$ and $(-, u)$ states is 1, while the $(-, g)$ and $(+, u)$ states have $g_{ns} = 0$. Therefore, the latter states do not appear in spectroscopic experiments on $^{12}C_2$. The MARVEL input set of measured transitions was checked for a corresponding labeling error.

2.4. Comments on the Data Sources

First, we make comments on those observed bands of C_2 which were not used in the MARVEL analysis.

The situation with the Deslandres–d’Azambuja band is a remarkable one. The band was originally observed more than a century ago (Deslandres & d’Azambuja 1905) and as discussed in the Introduction, it has been observed in a number of astronomical objects. However, while a high-resolution line list is available for $^{13}C_2$ (Antić-Jovanović et al. 1985) and there are a number of papers reporting laboratory observation of the band for $^{12}C_2$ (Herzberg & Sutton 1940; Hornbeck & Herman 1949; Cisak et al. 1969; Urdahl et al. 1988; Sorkhabi et al. 1997), there are no high resolution line data for the band. A high resolution re-measurement of the band for $^{12}C_2$ would be welcomed.

Observation of the Messerle–Krauss band is reported in a single, short paper (Messerle & Krauss 1967), which provides no line data. Similarly, there are so far no published lines for the recently detected Kable–Schmidt band (Nakajima et al. 2009).

The situation with the three Herzberg and two Goodwin–Cool VUV bands is somewhat different. There are papers reporting detailed spectra for each of these bands (Herzberg et al. 1969; Goodwin & Cool 1988b, 1989). However, each of them comes from a single uncorroborated measurement. As

these bands probe upper states that are too high in energy for reliable, independent theoretical predictions, it was decided to leave their inclusion in a MARVEL analysis for future work. We note that omitting the energy levels associated with these bands is not critical for the partition sums and thermodynamic data determined as part of this study.

We also note that papers by Sorkhabi et al. (1997) and, Joester et al. (2007) refer to the so-called LeBlanc band comprising weak $D \ ^1\Sigma_u^+ - B' \ ^1\Sigma_g^+$ transitions; however, we could find no line data on this band or any papers by LeBlanc reporting it.

Second, the set of comments below refer to data sources used in our MARVEL analysis and listed in Table 2.

- (2a) 06PeSi (Petrova & Sinita 2006). Uncertainty assumed to be 0.01 cm^{-1} (T. Petrova 2015, private communication).
- (2b) 04ChYeWoLi (Chan et al. 2004). The data used are extracted from 15ChKaBeTa (Chen et al. 2015).
- (2c) 97SoBILiXu (Sorkhabi et al. 1997) and 39Landsver (Landsverk 1939). Uncertainty of these two sources is assumed to be 1.0 and 0.2 cm^{-1} , respectively.
- (2d) 51Freymark (Freymark 1951). The stated uncertainty was doubled to 0.02 cm^{-1} , as this seems to be a more adequate guess of the accuracy of these transitions.
- (2e) 85YaCuMeCa (Yan et al. 1985). Results recorded using magnetic rotation. The data are provided by R. F. Curl (2015, private communication). The uncertainty was increased to 0.005 cm^{-1} , as values below this did not give consistent results during the MARVEL analysis.
- (2f) 85RoWaMiVe (Roux et al. 1985). This source presents an analysis of measurements by Amiot et al. (1979); the data were extracted from 15ChKaBeTa (Chen et al. 2015).
- (2g) 13BoSyKnGe (Bornhauser et al. 2013). New assignments and reassignments of the measurements by 13YeChWa (Yeung et al. 2013).
- (2h) 13YeChWa (Yeung et al. 2013). Assignments corrected following 13BoSyKnGe (Bornhauser et al. 2013).
- (2i) 03KaYaGuYu (Kaniki et al. 2003). 0.007 cm^{-1} uncertainty; includes 26 transitions with $\Delta\Omega = 1$.
- (2j) 85CuSa (Curtis & Sarre 1985), 85SuSaHi (Suzuki et al. 1985), 94PrBe (Prasad & Bernath 1994) and 10BoKnGe (Bornhauser et al. 2010). Data extracted from 13BrBeScBa (Brooke et al. 2013).
- (2k) 86HaWi (Hardwick & Winicur 1986). Data provided by J. L. Hardwick (2015, private communication).
- (2l) 98BrHaKoCr (Brockhinke et al. 1998). Uncertainty assumed to be 0.02 cm^{-1} .
- (2m) 16KrBaWeNa (Krechivska et al. 2016). Gives a single line position as part of the multiphoton spectroscopic measurement of the ionization energy of C_2 .

Third, the next set of comments refers to sources listed in Table 3; these were not used in our MARVEL analysis for reasons listed below.

- (3a) 82ErLaMa (Erman et al. 1982). This source contains lifetime data but no transition frequencies.
- (3b) 68MeMe (Meinel & Messerle 1968). No actual line data given in the paper but 11BoSyKnGe (Bornhauser et al. 2011) presents some lines reassigned from this work that are included in our data set, see Table 2.

Table 2
Experimental Transitions Available in the Literature for Several Band Systems of $^{12}\text{C}_2$ and Their Overall Characteristics, Including the Number of Measured (A) and Validated (V) Transitions (Trans.)

Tag	References	Range(cm^{-1})	Method	Trans (A/V)	Comments
Phillips A $^1\Pi_u-X^1\Sigma_g^+$					
15ChKaBeTa	Chen et al. (2015)	2372–8822	FTS	319/318	...
88DaAbPh	Davis et al. (1988a)	4012–6031	D-FTS	191/191	...
88DoNiBea	Douay et al. (1988a)	4067–7565	FTS	241/238	...
77ChMaMa	Chauville et al. (1977)	4371–11424	FTS	774/770	...
63BaRab	Ballik & Ramsay (1963b)	6312–14469	...	574/532	...
06PeSi	Petrova & Sinitsa (2006)	9405–9434	...	8/8	(2a)
04ChYeWoLi	Chan et al. (2004)	10719–14128	...	293/293	(2b)
13NaEn	Nakajima & Endo (2013)	13182–16825	LIF	77/73	...
Mulliken D $^1\Sigma_u^+-X^1\Sigma_g^+$					
39Landsver	Landsverk (1939)	43051–43473	CAE	171/167	(2c)
97SoBILiXu	Sorkhabi et al. (1997)	43062–43490	LIF	179/165	(2c)
95BILiSo	Blunt et al. (1995)	43224–43289	DL	9/8	...
Bernath B $^1\Delta_g-A^1\Pi_u$					
88DoNiBeb	Douay et al. (1988b)	1951–7152	FTS	507/507	...
16ChKaBeTa	Chen et al. (2016)	1900–8422	FTS	1001/1001	...
Bernath B' $^1\Sigma_g^+-A^1\Pi_u$					
88DoNiBeb	Douay et al. (1988b)	5025–8365	FTS	237/237	...
Freymark E $^1\Sigma_g^+-A^1\Pi_u$					
97SoBILiXu	Sorkhabi et al. (1997)	43510–43660	LIF	66/65	(2c)
51Freymark	Freymark (1951)	45069–48772	...	376/354	(2d)
Ballik–Ramsay b $^3\Sigma_g^- - a^3\Pi_u$					
15ChKaBeTa	Chen et al. (2015)	2102–9404	FTS	3510/3507	...
85YaCuMeCa	Yan et al. (1985)	3673–4040	...	356/352	(2e)
85RoWaMiVe	Roux et al. (1985)	4643–8488	...	1309/1298	(2f)
79AmChMa	Amiot et al. (1979)	4856–9895	...	2168/2139	...
88DaAbSa	Davis et al. (1988b)	4897–5706	D-FTS	382/365	...
06PeSi	Petrova & Sinitsa (2006)	9388–9450	...	80/80	...
11BoSyKnGe	Bornhauser et al. (2011)	22991–23031	...	8/8	...
Swan d $^3\Pi_g - a^3\Pi_u$					
13NaEn	Nakajima & Endo (2013)	12596–23497	LIF	168/168	...
14NaEn	Nakajima & Endo (2014)	13673–13877	LIF	150/141	...
13BoSyKnGe	Bornhauser et al. (2013)	13847–13927	...	23/23	(2g)
13YeChWa	Yeung et al. (2013)	13849–14128	HCD	276/273	(2h)
07TaHiAm	Tanabashi et al. (2007)	15149–23110	FTS	3853/3771	...
48Phillips	Phillips (1948a)	16151–44722	discharge	1181/1128	...
02TaAm	Tanabashi & Amano (2002)	16877–17113	HCD	356/352	...
03KaYaGuYu	Kaniki et al. (2003)	17731–17895	...	153/150	(2i)
85CuSa	Curtis & Sarre (1985)	17736–17941	Doppler-free	217/217	(2j)
94PrBe	Prasad & Bernath (1994)	17915–21315	Jet cooled	39/39	(2j)
83Amiot	Amiot (1983)	19354–20191	FTS	347/346	...
99LIEw	Lloyd & Ewart (1999)	19354–19511	...	138/138	...
85SuSaHi	Suzuki et al. (1985)	21101–21263	...	194/194	(2j)
10BoKnGe	Bornhauser et al. (2010)	21343–21427	...	23/23	(2j)
11BoSyKnGe	Bornhauser et al. (2011)	21389–23019	...	46/46	...
Fox–Herzberg e $^3\Pi_g - a^3\Pi_u$					
86HaWi	Hardwick & Winicur (1986)	33036–33492	...	100/100	(2k)
49Phillips	Phillips (1948b)	35092–42019	discharge	1833/1664	...
98BrHaKoCr	Brockhinke et al. (1998)	40205–40339	...	10/10	(2l)
Duck d $^3\Pi_g - c^3\Sigma_u^+$					
13ChYeWa	Chan et al. (2013)	12074–12499	HCD	221/210	...
13NaEn	Nakajima & Endo (2013)	13030–16136	LIF	513/513	...
14NaEn	Nakajima & Endo (2014)	13650–13889	LIF	205/196	...
07JoNaRe	Joester et al. (2007)	15007–17080	LIF	235/234	...
Krechivska–Schmidt $4^3\Pi_g - a^3\Pi_u$					
15KrBaTrNa	Krechivska et al. (2015)	47921–48327	REMPI	67/67	...
16KrBaWeNa	Krechivska et al. (2016)	46736	...	1/1	(2m)
Intercombination a $^3\Pi_u - X^1\Sigma_g^+$					
15ChKaBeTa	Chen et al. (2015)	3501–8306	FTS	32/32	...

Table 2
(Continued)

Tag	References	Range(cm ⁻¹)	Method	Trans (A/V)	Comments
Intercombination A ¹ Π _u -b ³ Σ _g ⁻					
15ChKaBeTa	Chen et al. (2015)	3940	FTS	1/1	...
Intercombination I ⁵ Π _g -a ³ Π _u					
11BoSyKnGe	Bornhauser et al. (2011)	21370–21447	FWM	68/68	...
Radi–Bornhauser ¹ Σ _u ⁺ – ¹ Σ _g ⁺					
15BoMaGo	Bornhauser et al. (2015)	21772–21839	FWM	57/57	...

Notes. Comments are given in Section 2.4. CAE = carbon arc emission, D-FTS = discharge FTS, DL = dye laser, FTS = Fourier Transform Spectroscopy, FWM = four-wave mixing, HCD = Hollow-Cathode Discharge source, LIF = Laser Induced Fluorescence, MD = Microwave Discharge, SJT = Supersonic Jet Technique, REMPI = resonance-enhanced multiphoton ionization.

Table 3
Experimental Papers with Either No Data or with Data Not Included in the Present MARVEL Analysis

Tag	Reference	Range(cm ⁻¹)	Method	Data	Comments
Phillips A ¹ Π _u -X ¹ Σ _g ⁺					
82ErLaMa	Erman et al. (1982)	No	(3a)
Swan d ³ Π _g -a ³ Π _u					
63CaGi	Callomon & Gilby (1963)	No	...
68MeMe	Meinel & Messerle (1968)	No	(3b)
68PhDa	Phillips & Davis (1968)	Yes	(3c)
88UrBaJa	Urdahl et al. (1988)	21,280–25,930	...	No	...
90ChMa	Chen & Mazumder (1990)	No	...
97KaHuEw	Kaminski et al. (1997)	No	(3d)
94CaDo	Caubet & Dorthe (1994)	No	(3e)
99LIEw	Lloyd & Ewart (1999)	Yes	(3f)
05SmPaSc	Smith et al. (2005)	...	CL	No	...
Ballik–Ramsay b ³ Σ _g ⁻ -a ³ Π _u					
63BaRaa	Ballik & Ramsay (1963a)	Yes	(3g)
D ¹ Σ _u ⁺ -B' ¹ Σ _g ⁺					
91BaUrJa	Bao et al. (1991)	28,030–28,555	LIF	No	...
Duck d ³ Π _g -c ³ Σ _u ⁺					
06KoReMoNa	Kokkin et al. (2006)	No	...
Kable–Schmidt e ³ Π _g -c ³ Σ _u ⁺					
09NaJoPaRe	Nakajima et al. (2009)	No	(3h)
Herzberg					
69HeLaMa	Herzberg et al. (1969)	69,000–73,000	FD	Yes	(3i)
Freyark E ¹ Σ _g ⁺ -A ¹ Π _u					
96BLiSo	Blunt et al. (1996)	43,510–43,545	LIF	No.	...
Deslandres–d'Azambuja C ¹ Π _g -A ¹ Π _u					
85AnBoPe	Antić-Jovanović et al. (1985)	23,800–31,250	E	...	(3j)
87VaHe	van de Burgt & Heaven (1987)	21,000–24,500	LIF	No	(3k)
88UrBaJa	Urdahl et al. (1988)	21,280–25,930	LIF	No	(3l)
Messerle–Krauss C' ¹ Π _g -A ¹ Π _u					
67MeKr	Messerle & Krauss (1967)	No	(3m)
Goodwin–Cool					
88GoCoa	Goodwin & Cool (1988a)	No	(3n)
88GoCob	Goodwin & Cool (1988b)	Yes	(3o)
89GoCo	Goodwin & Cool (1989)	Yes	(3p)

Note. Comments about these sources are given in Section 2.4. CL = chemiluminescence, E = emission, FD = flash discharge, LIF = laser-induced fluorescence.

- (3c) 68PhDa (Phillips & Davis 1968). A book with an extensive list of lines, including higher bands but only 3607 of the 10910 lines, could not be validated; Tanabashi & Amano (2002) also found that these assignments did not match those of other work. It was therefore decided to omit these lines from the final compilation.
- (3d) 97KaHuEw (Kaminski et al. 1997). A precursor to 99LIEw (Lloyd & Ewart 1999).

- (3e) 94CaDo (Caubet & Dorthe 1994). So-called HP band.
- (3f) 99LIEw (Lloyd & Ewart 1999). None of these data were selected by 13BrBeScBa (Brooke et al. 2013), so they were not considered in this study either.
- (3g) 63BaRaa (Ballik & Ramsay 1963a). Original observation by Ballik and Ramsay of their eponymous band. The work was re-assigned by Veseth (1975), but his results are not available.

- (3h) 09NaJoPaRe (Nakajima et al. 2009). Report of a new C_2 band but no data are provided and no follow-up study exists.
- (3i) 69HeLaMa (Herzberg et al. 1969). Report of three new VUV bands with line data. Upper states lie at too high energy for data to be validated.
- (3j) 85AnBoPe (Antić-Jovanović et al. 1985). Report of extensive data for $^{13}C_2$ but with no data set for $^{12}C_2$.
- (3k) 87VaHe (van de Burgt & Heaven 1987). Report of a “new” C_2 band: 25 transitions from one (unknown) band were recorded with an uncertainty of 0.2 cm^{-1} and assigned J quantum numbers; these were supplied by M. C. Heaven (2015, private communication). The calculations of Bruna & Wright (1992) suggest that this band actually belongs to C_2^+ rather than C_2 . The band remains unassigned and the data were not included in our current analysis.
- (3l) 88UrBaJa (Urdahl et al. 1988). No transition data reported in the paper.
- (3m) 67MeKr (Messerle & Krauss 1967). Discovery paper giving many spectroscopic parameters but no primary transition data.
- (3n) 88GoCoa (Goodwin & Cool 1988a). Discovery paper: follow-up work with data in 88GoCob (Goodwin & Cool 1988b) and 89GoCo (Goodwin & Cool 1989).
- (3o) 88GoCob (Goodwin & Cool 1988b). New band $1^1\Delta_u - A^1\Pi_u$ with line data. Upper states lie at too high energy for data to be validated.
- (3p) 89GoCo (Goodwin & Cool 1989). New band $1^1\Delta_u - B^1\Delta_g$ with line data. Upper states lie at too high energy for data to be validated.

2.5. Rovibronic Nuclear Motion Computations Using Duo

In order to decide on their correctness, we have compared the experimental MARVEL rovibronic energies with their theoretical counterparts. The latter approximate but complete set of energy levels is based on empirical PECs, spin-orbit curves (SOC), and electronic angular momentum curves (EAMC) of C_2 as given by Yurchenko et al. (2016b). The theoretical rovibronic energies were computed using a new diatomic nuclear motion program called Duo (Yurchenko et al. 2016a). Duo solves the fully coupled rovibronic Schrödinger equation variationally using a combination of discrete variable representation and rigid-rotor basis sets to represent the vibrational and the spin-rotational degrees of freedom in the Hund’s case (a) representation, respectively. The final PECs, SOCs, and EAMCs were obtained by refining *ab initio* curves obtained at the ic-MRCI/aug-cc-pVQZ level of electronic structure theory for the nine lowest electronic states of C_2 , $X^1\Sigma_g^+$, $A^1\Pi_u$, $B^1\Delta_g$, $B'^1\Sigma_g^+$, $a^3\Pi_u$, $b^3\Sigma_g^-$, $c^3\Sigma_u^+$, $d^3\Pi_g$, and $1^5\Pi_g$ — by fitting to the MARVEL energies. A detailed account of these computations will be reported elsewhere.

Duo uses the following quantum numbers motivated by the Hund’s case (a) choice of the basis set:

$$\{J, +/ -, \text{state}, v, \Lambda, \Sigma, \Omega\},$$

where Λ , Σ , and Ω ($\Omega = \Lambda + \Sigma$) are the signed quantum numbers corresponding to projections of the electronic, spin, and total angular momenta, respectively (the projection of the

rotational angular momentum \hat{R} on the molecular axis is zero). The Duo quantum numbers characterizing the computed rovibronic states are used to check and complete the MARVEL labels. It should be noted that Duo uses an approximate assignment scheme based on the largest contribution to the wavefunction expansion (Yurchenko et al. 2016a). Although this scheme is very robust, it can sometimes lead to ambiguous sets of quantum numbers, especially for states in strong resonance with other rovibronic states.

Comparison of the Duo and MARVEL results helped us to identify problems in the experimental data, such as misassigned lines, duplicate transitions, and outliers.

3. RESULTS AND DISCUSSION

3.1. Term Values

In its ground electronic state C_2 has a fairly strong bond (Mulliken 1939; Müller et al. 2001; Sherrill & Piecuch 2005b; Su et al. 2011). The equilibrium bond distance of the $X^1\Sigma_g^+$ state at 1.2425 \AA is short for a double bond (considerably shorter than the $C=C$ bond of ethylene at $r_e(C=C) = 1.331 \text{ \AA}$), but long for a triple bond (in C_2H_2 $r_e(CC) = 1.203 \text{ \AA}$). This also means that the dissociation energy of the $X^1\Sigma_g^+$ state is large, more than $50,000 \text{ cm}^{-1}$, in fact. Compared to this, the energy differences among the several feasible asymptotes comprised by the low-lying 3P , 1D , and 1S states of the C atom are relatively minor. Furthermore, the structure of the molecular orbitals (MO) of C_2 is such that a large number of low-energy singlet, triplet, and quintet valence states are feasible and many of them are part of experimentally measurable rovibronic transitions (see Table 1). In the $X^1\Sigma_g^+$ state the leading valence electron configuration is $(\text{core})(2\sigma_g)^2(2\sigma_u)^2(1\pi_u)^4$. By promoting electrons from the weakly antibonding $2\sigma_u$ and the strongly bonding $1\pi_u$ MOs and populating the $3\sigma_g$ MO a large number of electronic states arise. Fortunately, for obtaining proper, temperature-dependent ideal-gas thermochemical quantities up to about 4000 K, it is sufficient to consider nine electronic states, four singlet, four triplet, and one quintet states (see Table 4). As mentioned already, all these lowest-energy electronic states correlate with the $C(^3P) + C(^3P)$ separated-atom limit.

Not too surprisingly for such a simple molecule, a large number of electronic structure computations are available for C_2 in the literature (Kirby & Liu 1979; Bauschlicher & Langhoff 1987; Watts & Bartlett 1992; Boggio-Pasqua et al. 2000; Bruna & Grein 2001; Müller et al. 2001; Abrams & Sherrill 2004; Sherrill & Piecuch 2005a; Jiang & Wilson 2011; Boschen et al. 2013, 2014). There are several issues that make the electronic structure computations extremely challenging for C_2 . First, there is a quasi-degeneracy of the fully occupied $1\pi_u$ and the empty $3\sigma_g$ MOs, explaining some of the unusual characteristics of the excited electronic states of C_2 . Second, the existence of several low-lying excited electronic states leads to the occurrence of a considerable number of avoided crossings among the PECs as the CC distance is varied. Third, as pointed out by Abrams & Sherrill (2004) based on full configuration interaction computations, at least in the cases of the X, B, and B’ states, methods based on an unrestricted Hartree–Fock (UHF) reference provide correct but methods based on a restricted HF (RHF) reference provide

Table 4Empirical, Experimental (MARVEL), and Theoretical T_e and T_0 Term Values, in cm^{-1} , of the Six Lowest-energy Singlet and Triplet and the Two Lowest-energy Quintet Electronic States of C_2

State	T_e			T_0			
	Calc. ^a	Empirical	Duo ^b	Empirical	MARVEL ^{b,c}	J	F
X $^1\Sigma_g^+$	0.0	0.0	0.0	0.0	0.0	0	1
a $^3\Pi_u$	509	720.0083(21) ^d	722.58	603.828 ^e	603.817(5)	2	1
b $^3\Sigma_g^-$	6233	6439.08382(58) ^d	6437.00	6250.164 ^e	6250.149(7)	0	3
A $^1\Pi_u$	8374	8391.4062(19) ^d	8393.63	8271.606 ^e	8271.607(7)	1	1
c $^3\Sigma_u^+$	9371	9124.2 ^f	9172.30	9277 ^g	9280.215(5)	1	2
B $^1\Delta_g$	11966	12082.34355(54) ^h	12092.45	11859 ^g	11867.825(5)	2	1
B' $^1\Sigma_g^+$	15261	15410.33(36) ^h	15401.52	15197 ^g	15196.509(5)	0	1
d $^3\Pi_g$	20092	20022.5 ^f	20030.92	19992 ^g	19983.953(8)	2	1
1 $^5\Pi_g$	29258.5922(48) ⁱ	29860.921(5)	2	1
e $^3\Pi_g$...	40796.7 ^f	40422.691(50)	2	1
D $^1\Sigma_u^+$...	43239.8 ^f	43230.499(138)	1	1
1 $^5\Pi_u$	51 049.799 ^j	51651.142(20)	1	1
4 $^3\Pi_g$	52106.042(94)	1	1
E $^1\Sigma_g^+$...	55034.7 ^f	54936.672(150)	0	1

Notes.^a Müller et al. (2001), MR-CISD values at the complete basis set (CBS) limit.^b This work.^c The lowest observed energy level in each electronic state is reported. J and F are the quantum numbers of this level.^d From Chen et al. (2015).^e Vibronic energies taken from the supplementary material of Chen et al. (2015).^f From Babou et al. (2009).^g Empirical vibronic energies taken from Chen et al. (2015).^h From Chen et al. (2016).ⁱ From Bornhauser et al. (2011), relative to the $\nu = 0$ level of the a $^3\Pi_u$ state.^j From Bornhauser et al. (2015), relative to the $\nu = 0$ level of the a $^3\Pi_u$ state.**Table 5**Vibrational Energy Levels of the X $^1\Sigma_g^+$, B' $^1\Sigma_g^+$, and E $^1\Sigma_g^+$ States of C_2

State	ν	Calc. ^a	Expt. ^b	MARVEL ^c
X $^1\Sigma_g^+$	1	1829.15	1827.4849(2)	1827.486(5)
	2	3630.35	3626.6835(2)	3626.681(10)
	3	5402.78	5396.6892(4)	5396.686(9)
	4	7145.40	7136.3507(6)	7136.350(6)
	5	8856.84	8844.1241(11)	8844.124(7)
	6	10536.37	10517.9659(39)	10517.950(7)
	7	12178.69	12154.9615(29)	12154.961(6)
	8	13783.76	13751.3944(38)	13751.393(3)
	9	15346.69	15302.8952(46)	15302.893(7)
B' $^1\Sigma_g^+$	1	...	1420.4850(4)	1420.488(9)
	2	...	2840.0048(4)	...
	3	...	4261.0686(4)	4261.071(1)
	4	...	5681.5113(6)	...
E $^1\Sigma_g^+$	1	1592.316(200)

Notes. All values are given in cm^{-1} . All energies are relative to the appropriate $\nu = 0$ vibrational level.^a From 07KoBaSc (Kokkin et al. 2007).^b From Chen et al. (2016).^c This work, values of the $\nu = 0$ vibrational levels of X $^1\Sigma_g^+$, B' $^1\Sigma_g^+$, and E $^1\Sigma_g^+$ are, in cm^{-1} , 0.0, 15196.509, and 54936.664, respectively.

incorrect results. Fourth, one must account for the strong multireference character of the electronic states and the near degeneracies changing rapidly along the CC distance. Fifth, rather large atom-centered, fixed-exponent Gaussian basis sets are required for the correct and converged description of the

Table 6The Lowest-energy States with $J \neq 0$ of the Excited Vibrational Levels of the A $^1\Pi_u$ and B $^1\Delta_g$ Singlet States of C_2

State	ν	J	MARVEL ^a	State	ν	J	MARVEL ^a
A $^1\Pi_u$	1	1	1584.008(4)	B $^1\Delta_g$	1	2	1384.440(2)
		2	3143.805(5)			2	2746.010(9)
		3	4679.323(6)			3	2746.010(9)
		4	6190.503(7)			4	5400.804(8)
		5	7677.273(4)			5	6694.148(10)
		6	9139.523(9)			6	7964.836(3)
		7	10577.184(13)			7	9214.047(3)
		8	...			8	10446.668(5)
		9	13378.377(1)		
		10	14741.688(1)		
		11	16079.978(7)		
		12	17393.116(8)		
		13	18680.944(7)		
		14	19943.297(7)		
		15	21179.968(7)		
		16	22390.754(7)		

Notes. All values are given in cm^{-1} . All energies are relative to the appropriate $\nu = 0$ vibrational level.^a J is the quantum number corresponding to the total angular momentum. The values of the $\nu = 0$ vibrational levels of A $^1\Pi_u$ and B $^1\Delta_g$ are $8271.607(7) \text{ cm}^{-1}$ ($J = 1$) and $11867.825(5) \text{ cm}^{-1}$ ($J = 2$), respectively. The rule $J \geq |\Omega|$ for Hund's case (a) coupling explains the lack of the $J = 0$ states for A $^1\Pi_u$ and the $J = 0, 1$ states for B $^1\Delta_g$.

valence states. These difficulties explain why this deceptively simple diatomic molecule is still one of the favorites of developers of modern wavefunction-based electronic structure

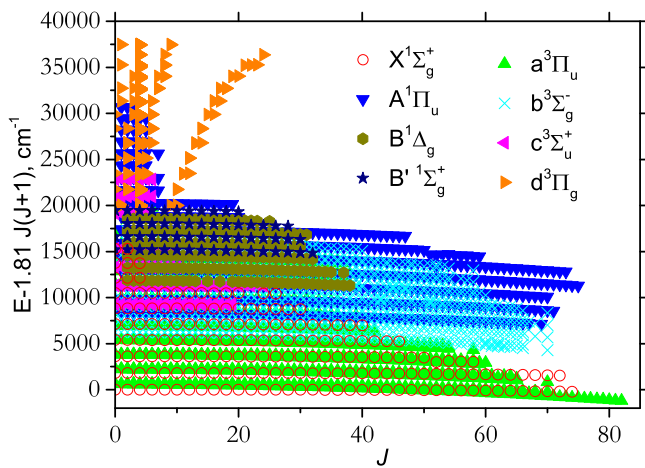


Figure 3. The MARVEL term values for the eight lowest-energy singlet and triplet states shown as a reduced-energy diagram, after subtraction of $1.81J(J+1) \text{ cm}^{-1}$ from the energy E of the state.

techniques (Watts & Bartlett 1992; Müller et al. 2001; Boschen et al. 2013).

Using CI methods, 27 bound valence states of C_2 were computed by Fougere & Nesbet (1966). Kirby & Liu (1979) obtained results for all 62 electronic states in the valence manifold, including weakly bound and repulsive ones. Pouilly et al. (1983) obtained results for Rydberg states, as well. Electronic states with T_e values up to $75,000 \text{ cm}^{-1}$ (this is in fact the $F^1\Pi_u$ state) have been studied, but for the present investigation the energy cut-off value was chosen to be $35,000 \text{ cm}^{-1}$. This limits the number of singlet, triplet, and quintet states to 4, 4, and 1, respectively, 9 states altogether. None of the higher-lying states will be considered in what follows. Note that RKR potential curves are given for several singlet, triplet, and quintet states in Martin (1992).

In this study, the so-called T_0 values obtained for the electronic states define directly the lowest measurable term energies of the states (thus, they may not necessarily correspond to $J=0$). It is not that simple to determine the T_e values of the excited electronic states of C_2 , as these are not measurable quantities. This can only be achieved if the zero-point vibrational energy of all the states is determined. However, since all states are coupled in the Duo computations, these do not come directly from our joint MARVEL and Duo analysis. In particular, for the singlet Π and Δ electronic states there are no transitions to $J=0$ upper rovibronic states.

3.2. Vibrational Energy Levels

Figure 3 shows all MARVEL term values below $35,000 \text{ cm}^{-1}$ for four singlet and four triplet states, where $1.81J(J+1) \text{ cm}^{-1}$ has been subtracted from the computed energies to make the figure clearer: this means that near-horizontal sequences of levels for a particular electronic state are all associated with something one could call a single vibrational level. Figure 3 shows that the largest total angular momentum quantum numbers, J_{max} , are 74, 75, 86, and 70 for the $X^1\Sigma_g^+$, $A^1\Pi_u$, $a^3\Pi_u$, and $b^3\Sigma_g^-$ states, respectively. As expected, as the vibrational excitation increases, the J_{max} value usually decreases. Finally, note that the coverage of rovibronic levels up to $35,000 \text{ cm}^{-1}$ from experiment is not complete; assuming rigid rotation, data up to about $J=144$ are needed to

Table 7

Excited Vibronic Levels for the Four Lowest-energy Triplet States of C_2 with $J=0$ and F_3

State	ν	MARVEL ^a
a $^3\Pi_u$	1	1617.985(10)
	2	3212.620(9)
	3	4783.940(5)
	4	6331.973(1)
	5	7855.893(100)
	7	10835.820(1)
	8	12290.393(1)
	9	13721.623(5)
	10	15129.564(1)
	11	16514.369(1)
	b $^3\Sigma_g^-$	1
2		2874.028(2)
3		4277.927(1)
5		9859.060(1)
c $^3\Sigma_u^+$	1	2031.833(8)
	2	4034.776(7)
	3	6007.745(8)
	5	9859.060(1)
	6	11734.338(10)
	7	13573.601(1)
	10	15245.388(2)
d $^3\Pi_g$	1	1753.500(7)
	2	3469.636(10)
	3	5145.247(6)
	4	6776.153(1)
	5	8356.139(7)
	6	9880.362(7)
	7	11337.658(1)
	8	12722.024(1)
	9	14025.567(1)
	10	15245.388(2)

Notes. All values are given in cm^{-1} . Energies in each electronic state are relative to the appropriate $\nu=0$ ($J=0$, F_3) vibrational level.

^a The ($\nu=0$, $J=0$, F_3) energy values are 632.730, 6250.149, 9280.834, and 20009.011 for the a $^3\Pi_u$, b $^3\Sigma_g^-$, c $^3\Sigma_u^+$, and d $^3\Pi_g$ states, respectively.

have full coverage of the energy levels required during the thermochemical analysis. This coverage is provided in this study by Duo energy levels (vide infra).

Due to the strength of the CC bond in all the electronic states studied, the vibrational fundamental is substantial in almost all the bound electronic states of C_2 . In fact, for the ground electronic state the harmonic wavenumber is close to 2000 cm^{-1} , a high value for a relatively heavy molecule. Thus, the number of vibrational states is not that high, despite the large dissociation energy. In particular, Boschen et al. (2013) computed 57, 54, 49, and 36 bound vibrational levels for the $X^1\Sigma_g^+$, $A^1\Pi_u$, $B^1\Delta_g$, and $B'^1\Sigma_g^+$ states, respectively. The number of vibrational levels characterized by our MARVEL analysis is considerably smaller, only 9, 16, 8, and 3, respectively. The vibrational energies presented for the triplet electronic states given in Table 7 cannot be compared easily with existing literature values, since the MARVEL values are for a specific spin component of a rovibronic energy level.

The largest “vibrational fundamental” ($J=0$) corresponding to the electronic states studied here is that of the c $^3\Sigma_u^+$ state, at 2031.833 cm^{-1} . Consequently, this state must have the strongest CC bond.

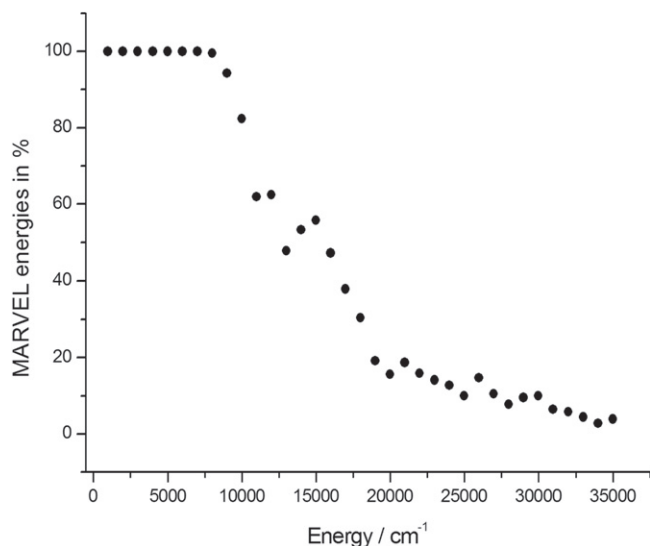


Figure 4. Completeness of the rovibronic MARVEL energies as a function of the excitation energy.

3.3. Rovibrational Energy Levels

The rotational constant of C_2 for the $X^1\Sigma_g^+$ state is relatively small, about 1.81 cm^{-1} . This results in a large number of rotational states for each vibrational level. As part of this study, DUO results were obtained up to $J = 144$. They served to check whether a MARVEL energy level is viable or not and they were generated to help the thermochemical analysis of this study (vide infra).

The lowest missing MARVEL energy level is at 7800 cm^{-1} ; up to this energy the coverage is complete. As Figure 4 shows, as the energy increases there are more and more experimentally unknown energy levels. The coverage drops below 10% at about $30,000\text{ cm}^{-1}$.

It is interesting to note how close some of the rovibrational energy differences are to each other. Take the $^3\Pi_u$ state as an example. The $v = 1 - v = 0$ energy difference for $J = 0$ is 1617.985 cm^{-1} . The highly similar energy differences for the different spin components ($J = 1, F = 2$), ($J = 1, F = 3$), ($J = 2, F = 1$), ($J = 2, F = 2$), and ($J = 2, F = 3$), are 1618.063 , 1617.941 , 1617.985 , 1617.902 , and 1617.831 , respectively. The reason behind this observation is that each spin component of each vibrational level of the $^3\Pi_u$ state has a slightly different effective value for their rotational constant due to both electronic and vibrational effects, and these energy differences include rotational energies. The first-principles DUO energies, where such interactions are taken explicitly into account, result in similar energy differences.

4. THERMOCHEMICAL PROPERTIES OF C_2

Altman (1960) and Clementi (1961) seem to be the first to address the thermochemical properties of the C_2 molecule. They both based their analyses on spectroscopic constants available to them and included several, but not all necessary, electronic states in their study. More recent thermochemical studies include those by Irwin (1981), Sauval & Tatum (1984), and Rossi et al. (1985). The most reliable results appear to have been given by Gurvich & Veys (1990).

The internal partition function, $Q_{\text{int}}(T)$, of C_2 is computed here via the direct summation recipe (Vidler & Tennyson 2000)

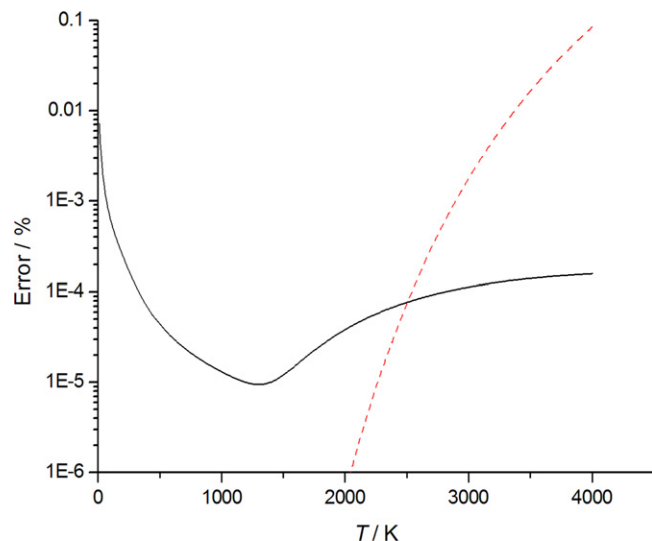


Figure 5. Sources of uncertainty in the internal partition function of $^{12}C_2$ up to 4000 K. The solid (black) line shows the uncertainty that arises from the uncertainties of the known energy levels. The dashed (red) curve represents the convergence error, in percent, due to energy levels not included in the analysis.

using a mixture of experimental (MARVEL) and theoretical (DUO) energy levels. DUO provides the full set of energies for the nine electronic states considered during the determination of the ideal-gas thermochemistry of C_2 . While this is a complete set, the energy levels are of limited accuracy. Thus, whenever possible, the DUO energy levels are replaced by the incomplete but accurate set of MARVEL rovibronic energies. The final energies are used to compute the internal partition sum, its first (Q') and second (Q'') moments, and the isobaric specific heat capacity (C_p) as a function of temperature.

Inaccuracies in $Q_{\text{int}}(T)$ have three sources of origin. The first is the intrinsic uncertainty of the energy levels. The second is the lack of a complete set of bound rovibronic energy levels. The third is associated with the treatment, including the possible neglect, of the unbound states.

The main source of uncertainty in $Q_{\text{int}}(T)$ can be estimated straightforwardly using the uncertainty of each energy level and an error propagation formula. All experimental (MARVEL) energy levels have an associated uncertainty, while an uncertainty of 5.0 cm^{-1} was assumed for the uncertainties of all the DUO levels. (Note that this uncertainty estimate is rather pessimistic.) Figure 5 (solid line) shows the impact of the uncertainties of the energy levels on the uncertainty of $Q_{\text{int}}(T)$. It can be seen that up to about 2500 K this type of uncertainty is dominant, but its maximum value, occurring at the lowest temperatures, is still less than 0.01%. Estimation of the second type of error is hard since (a) the exact number of the energy levels is unknown, and (b) the value of the partition function grows monotonically as more and more energy levels are considered in the direct sum. Therefore, only an approximate convergence can be reached at higher temperatures during the direct summation. To check the convergence of the partition function we need a larger set of energy levels; therefore, we computed approximate rovibronic energy levels for all the electronic states considered, using the spectroscopic constants published by Gurvich & Veys (1990) up to $70,000\text{ cm}^{-1}$. Using the spectroscopic constants of 27 electronic states we could determine 332 347 extra energy levels above $35,000\text{ cm}^{-1}$. Figure 5 (dashed line) shows the difference

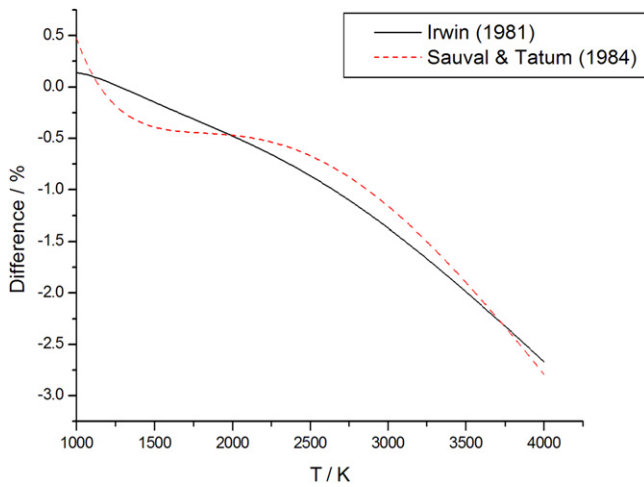


Figure 6. The percentage differences of our partition function from Irwin (1981; solid, black) and from Sauval & Tatum (1984; dashed, red).

(in percent) of the two data sets, (MARVEL + DUO) and (MARVEL + DUO + approximate energy levels). Although up to 2000 K the partition function is fully converged (the difference is less than $10^{-6}\%$), above 2000 K the difference begins growing appreciably. Nevertheless, the maximum uncertainty is still less than 0.1% at 4000 K, which is acceptable for probably all practical applications. In the case of C_2 , no consideration of unbound states (Szidarovszky & Császár 2015) is necessary, due to the large dissociation energy of C_2 .

The Q , Q' , Q'' , and C_p results are given in Table 10 in 100 K intervals. The full set of results at 1 K increments is given in the machine readable version of the table in the electronic edition.

Figure 6 shows the result of the comparison of our $Q_{\text{int}}(T)$ with those of Irwin (1981) and Sauval & Tatum (1984). It can be seen that the earlier studies always yield smaller numbers for the partition function of C_2 than the present study. A possible explanation is that we use a larger (more complete) set of energy levels. Note that the temperature range of the two earlier works begins from 1000 K.

Figure 7 shows the difference between our C_p results and the JANAF (Chase et al. 1985), Gurvich & Veyts (1990), ESA (Capitelli et al. 2005), and Altman (1960) and Clementi (1961) data. Altman (1960) reported C_p values from 0 to 6000 K, but Clementi (1961) corrected his values above 2000 K. While there is good agreement with the ESA and Altman & Clementi data at low temperatures, the difference begins to increase with the temperature. Conversely, for Gurvich and JANAF, the differences, especially compared to those of Gurvich & Veyts, are surprisingly large at lower temperatures. Babou et al. (2009) also found this discrepancy concerning the Gurvich & Veyts (NASA) data at lower temperatures; nevertheless, they could not explain this strange behavior. We believe that the problem originates from the incorrect usage of T_e values in Gurvich & Veyts (1990). The standard (spectroscopic) energy expansions use T_e as a minimum-to-minimum excitation energy; in this case the rovibronic energy levels of the upper electronic state will be shifted by the difference of the zero-point energies, by about $0.5 \Delta\omega_e$. To get the correct energies, the T_0 values should be used instead of the T_e values. The first excited electronic state usually lies above the ground state; therefore, this relatively small shift does not cause a significant

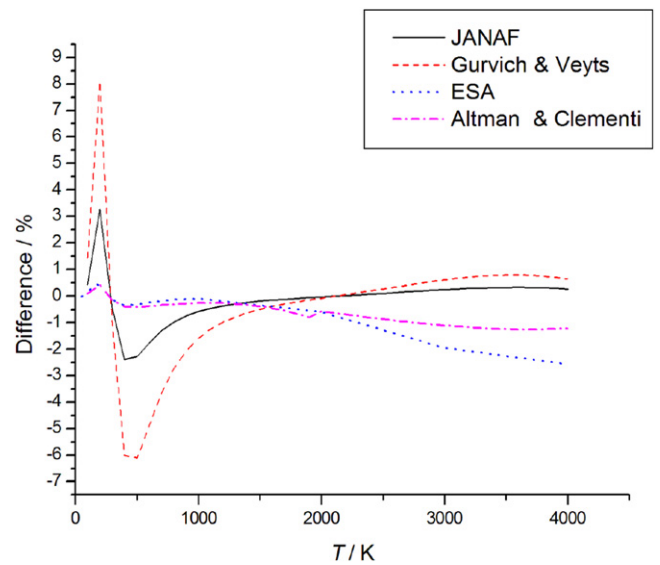


Figure 7. Comparison of our C_p results with JANAF (Chase et al. 1985) (solid), Gurvich & Veyts (1990) (dashed), ESA (Capitelli et al. 2005) (dotted), and Altman (1960) & Clementi (1961) (dashed-dotted, see text) values.

Table 8
Coefficients of the Fit (see Equation (3)), to the Internal Partition Function of $^{12}C_2$

Coefficient	0–200 K	201–4000 K
a_0	3.6577362306	186.8558092069
a_1	-7.0625294443	-139.9034556834
a_2	5.4057108902	42.4445304374
a_3	-2.0744319852	-6.6283715970
a_4	0.4447612738	0.5612382751
a_5	-0.0504276952	-0.0241572167
a_6	0.0023610646	0.00040521942

problem if left out of consideration. However, in the case of C_2 , where the relative energy of the a $^3\Pi_u$ state is smaller than the vibrational fundamental of either state, the incorrect use of T_e leads to wrong C_p values at lower temperatures.

Table 8 gives coefficients of the least squares fit to our computed partition function using the traditional form of Vidler & Tennyson (2000)

$$\log Q_{\text{int}} = \sum_{i=0}^6 a_i (\log T)^i. \quad (3)$$

In order to get the best reproduction of the directly computed values, the fit had to be performed in two separate temperature ranges. The first range is 0–200 K, the other is 201–4,000 K. These fits can reproduce the values of $\log Q$ reasonably accurately, within 0.1% in either region. Nevertheless, to take full advantage of the high accuracy of the present thermochemical results for C_2 , the numerical results of the Supplementary Information should be used. This supplementary information also contains the transitions file that forms the input for MARVEL, and that can be augmented with any future spectroscopic data on C_2 and rerun, and the associated energies file that is the output from the MARVEL run.

Table 9
Temperature-dependent Thermochemical Data for $^{12}\text{C}_2$

T/K	$Q_{\text{int}}(T)$	$Q'_{\text{int}}(T)$	$Q''_{\text{int}}(T)$	$C_p(T)/\text{J K}^{-1} \text{mol}^{-1}$
100.0	19.3786(1)	19.3839(8)	40.242(8)	29.7333(2)
200.0	41.6629(1)	55.1971(7)	170.867(15)	40.2915(2)
300.0	78.0529(1)	137.7708(7)	453.195(28)	43.1578(2)
400.0	133.6964(1)	260.3942(7)	812.605(39)	39.7816(2)
500.0	207.5463(1)	411.2436(7)	1225.949(48)	37.2546(2)
600.0	297.5930(1)	585.6218(7)	1700.047(59)	36.0862(2)
700.0	402.3796(1)	782.8055(7)	2244.006(70)	35.6865(2)
800.0	521.0433(1)	1003.3874(7)	2863.969(87)	35.6538(2)
900.0	653.1204(1)	1248.2596(7)	3564.19(15)	35.7888(2)
1000.0	798.3910(1)	1518.3519(7)	4348.50(38)	36.0006(2)
1100.0	956.7878(1)	1814.6138(7)	5221.04(92)	36.2499(2)
1200.0	1128.3464(1)	2138.0495(7)	6186.5(19)	36.5204(3)
1300.0	1313.1770(1)	2489.7472(7)	7250.5(37)	36.8053(5)
1400.0	1511.4500(2)	2870.8933(7)	8418.9(65)	37.1015(7)
1500.0	1723.3857(2)	3282.7725(13)	9698(10)	37.4068(10)
1600.0	1949.2475(3)	3726.7596(19)	11095(15)	37.7195(14)
1700.0	2189.3369(4)	4204.3059(28)	12616(22)	38.0375(17)
1800.0	2443.9883(6)	4716.9251(38)	14269(30)	38.3585(21)
1900.0	2713.5652(8)	5266.1783(51)	16060(41)	38.6803(25)
2000.0	2998.4562(11)	5853.6614(65)	17996(53)	39.0006(29)
2100.0	3299.0714(15)	6480.9933(83)	20084(66)	39.3173(33)
2200.0	3615.8393(19)	7149.806(11)	22332(81)	39.6285(36)
2300.0	3949.2042(24)	7861.740(17)	24744(98)	39.9326(40)
2400.0	4299.6233(32)	8618.434(34)	27329(116)	40.2281(43)
2500.0	4667.5647(49)	9421.521(74)	30092(135)	40.5139(50)
2600.0	5053.5054(88)	10272.63(15)	33039(156)	40.7893(63)
2700.0	5457.929(17)	11173.38(32)	36178(178)	41.0535(92)
2800.0	5881.327(33)	12125.37(63)	39513(201)	41.306(14)
2900.0	6324.193(64)	13130.2(12)	43051(225)	41.546(23)
3000.0	6787.02(11)	14189.4(21)	46798(251)	41.775(36)
3100.0	7270.32(21)	15304.7(36)	50760(280)	41.991(56)
3200.0	7774.59(36)	16477.4(60)	54941(316)	42.195(83)
3300.0	8300.33(61)	17709.2(98)	59348(363)	42.38(12)
3400.0	8848.04(98)	19001(15)	63986(429)	42.56(17)
3500.0	9418.2(15)	20355(23)	68859(528)	42.73(23)
3600.0	10011.4(23)	21773(35)	73971(673)	42.89(32)
3700.0	10628.0(35)	23256(52)	79328(882)	43.03(42)
3800.0	11268.6(52)	24805(74)	84933(1172)	43.16(56)
3900.0	11933.7(75)	26421(105)	90789(1562)	43.28(71)
4000.0	12624(11)	28106(146)	96899(2076)	43.39(91)

Note. The uncertainties associated with the data are given in parentheses.

(This table is available in its entirety in machine-readable form.)

5. SUMMARY

This study utilizes the MARVEL technique to accurately determine close to 6000 experimental rovibronic energies of $^{12}\text{C}_2$ for six singlet, six triplet, and two quintet electronic states, including the eight lowest valence states, which gives coverage up to $35,000 \text{ cm}^{-1}$. We survey all available laboratory high-resolution spectroscopic studies to provide input data for this process, resulting in 23,343 transitions connecting the 14 electronic states. While there are many spectroscopic studies available, 42 were analyzed to yield the transitions analyzed, and there has been significant recent activity, including the identification of several new band systems, there are also surprising gaps. For example, there is a detailed, fully rovibronically resolved study of the Deslandres–d’Azambuja ($\text{C } ^1\Pi_g\text{--A } ^1\Pi_u$) band system for $^{13}\text{C}_2$ (Antić-Jovanović et al. 1985), but even a century after the original observation of this band (Deslandres & d’Azambuja 1905) there is no available high-resolution study for $^{12}\text{C}_2$.

The recent observation of singlet–triplet intercombination bands by Chen et al. (2015) helped us to achieve linking all rovibronic levels of $^{12}\text{C}_2$ into a single huge component within its experimental SN; thus, individual intercombination lines can now be predicted accurately using the results of our study. This is a significant step toward the astronomical detection of these transitions (Lebourlot & Roueff 1986). To further aid this work and other astronomical studies involving C_2 , a full rovibronic line list for $^{12}\text{C}_2$ is currently being constructed using the variational code Duo by Yurchenko et al. (2016b), as part of the ExoMol project (Tennyson & Yurchenko 2012).

As of now, the full set of MARVEL results comprising a file of validated transition frequencies and a file containing the resulting rovibronic energy levels is given in the supplementary information of this paper. The highly accurate but limited set of experimental (MARVEL) energy levels augmented with the much less accurate but much more complete set of Duo energy levels has been used to compute ideal-gas thermochemical

functions for $^{12}\text{C}_2$ up to 4000 K. The accuracy of the partition function is better than 0.1% even at the highest temperatures, considerably exceeding the accuracy of all previous studies. This assures that the accuracy of the present isobaric heat capacity of $^{12}\text{C}_2$ is significantly better than that of any previous study.

We thank Robert Curl, John Hardwick, Michael Heaven, and Jian Tang for supplying the (unpublished) data from their spectroscopic experiments, and Tatiana Petrova and Peter Radi for comments on their data. Peter Radi is also thanked for his comments on the manuscript. This work has received support from the European Research Council under Advanced Investigator Project 267219, and the Scientific Research Fund of Hungary (grant OTKA NK83583). Collaboration of the UCL and ELTE groups has greatly benefited from the support of two COST actions, CoDECS (CM1002) and MOLIM (CM1405). Some funding was provided by the NASA Laboratory Astrophysics Program.

REFERENCES

- Abrams, M. L., & Sherrill, C. D. 2004, *JChPh*, **121**, 9211
- Al Derzi, A. R., Furtenbacher, T., Yurchenko, S. N., Tennyson, J., & Császár, A. G. 2015, *JQSRT*, **161**, 117
- Altman, R. L. 1960, *JChPh*, **32**, 615
- Amiot, C. 1983, *ApJS*, **52**, 329
- Amiot, C., Chauville, J., & Maillard, J.-P. 1979, *JMoSp*, **75**, 19
- Angeli, C., Cimiraaglia, R., & Pastore, M. 2012, *MolPh*, **110**, 2963
- Antić-Jovanović, A., Bojović, V., Pesić, D. S., et al. 1985, *JMoSp*, **110**, 86
- Asplund, M., Grevesse, N., Sauval, A. J., Prieto, C. A., & Blomme, R. 2005, *A&A*, **431**, 693
- Babou, Y., Riviere, P., Perrin, M.-Y., & Soufiani, A. 2009, *IJT*, **30**, 416
- Ballik, E. A., & Ramsay, D. A. 1958, *JChPh*, **29**, 1418
- Ballik, E. A., & Ramsay, D. A. 1959, *JChPh*, **31**, 1128
- Ballik, E. A., & Ramsay, D. A. 1963a, *ApJ*, **137**, 61
- Ballik, E. A., & Ramsay, D. A. 1963b, *ApJ*, **137**, 84
- Bao, Y., Urdahl, R. S., & Jackson, W. M. 1991, *JChPh*, **94**, 808
- Bauschlicher, C. W., & Langhoff, S. R. 1987, *JChPh*, **87**, 2919
- Bernath, P. F. 2016, *Spectra of Atoms and Molecules* (3rd ed.; Oxford: Oxford Univ. Press)
- Bleekrode, R., & Nieuwpoort, W. C. 1965, *JChPh*, **43**, 3680
- Blunt, V. M., Lin, H., Sorkhabi, O., & Jackson, W. M. 1995, *JMoSp*, **174**, 274
- Blunt, V. M., Lin, H., Sorkhabi, O., & Jackson, W. M. 1996, *CPL*, **257**, 347
- Boggio-Pasqua, M., Voronin, A., Halvick, P., & Rayez, J. 2000, *JMoSt (THEOCHEM)*, **531**, 159
- Booth, G. H., Cleland, D., Thom, A. J. W., & Alavi, A. 2011, *JChPh*, **135**, 084104
- Bornhauser, P., Knopp, G., Gerber, T., & Radi, P. P. 2010, *JMoSp*, **262**, 69
- Bornhauser, P., Marquardt, R., Gourlaouen, C., et al. 2015, *JChPh*, **142**, 094313
- Bornhauser, P., Sych, Y., Knopp, G., Gerber, T., & Radi, P. P. 2011, *JChPh*, **134**, 044302
- Bornhauser, P., Sych, Y., Knopp, G., Gerber, T., & Radi, P. P. 2013, *CPL*, **572**, 16
- Boschen, J. S., Theis, D., Ruedenberg, K., & Windus, T. L. 2013, *Theor. Chem. Acc.*, **133**, 1425
- Boschen, J. S., Theis, D., Ruedenberg, K., & Windus, T. L. 2014, *Theor. Chem. Acc.*, **133**, 1425
- Brault, J. W., Delbouille, L., Grevesse, N., et al. 1982, *A&A*, **108**, 201
- Brewer, L., & Hagan, L. 1979, *HTemS*, **11**, 233
- Brockhinke, A., Hartlieb, A. T., Kohse-Hoinghaus, K., & Crosley, D. R. 1998, *ApPhB*, **67**, 659
- Brooke, J. S., Bernath, P. F., Schmidt, T. W., & Bacskay, G. B. 2013, *JQSRT*, **124**, 11
- Brown, J., & Carrington, A. 2003, *Rotational Spectroscopy of Diatomic Molecules* (Cambridge: Cambridge Univ. Press)
- Bruna, P., & Grein, F. 2001, *CalPh*, **79**, 653
- Bruna, P. J., & Wright, J. S. 1992, *JPhCh*, **96**, 1630
- Callomon, J. H., & Gilby, A. C. 1963, *CalPh*, **41**, 995
- Capitelli, M., Colonna, G., Giordano, D., et al. 2005, *Tables of Internal Partition Functions and Thermodynamic Properties of High-Temperature Mars-Atmosphere Species from 50 K to 50000 K*, Tech. Rep., ESA Scientific Technical Review (Noordwijk: ESA)
- Caubet, P., & Dorthe, G. 1994, *CPL*, **218**, 529
- Chan, M.-C., Yeung, S.-H., Wang, N., & Cheung, A. S.-C. 2013, *JPCA*, **117**, 9578
- Chan, M.-C., Yeung, S.-H., Wong, Y.-Y., et al. 2004, *CPL*, **390**, 340
- Chase, M. W., Davies, A. C., Downey, J. R., et al. 1995, *JPCRD*, **14**, Suppl.
- Chauville, J., Maillard, J. P., & Mantz, A. W. 1977, *JMoSp*, **68**, 399
- Chen, W., Kawaguchi, K., Bernath, P. F., & Tang, J. 2015, *JChPh*, **142**, 064317
- Chen, W., Kawaguchi, K., Bernath, P. F., & Tang, J. 2016, *JChPh*, **144**, 064301
- Chen, X., & Mazumder, J. 1990, *ApPhL*, **57**, 2178
- Cisak, H., Dabrowska, K., & Rytel, M. 1969, *AcPP*, **36**, 497
- Clementi, E. 1961, *ApJ*, **133**, 303
- Császár, A. G., & Furtenbacher, T. 2011, *JMoSp*, **266**, 99
- Császár, A. G., Furtenbacher, T., & Árendás, P. 2016, *JPCA*, submitted
- Curtis, M., & Sarre, P. 1985, *JMoSp*, **114**, 427
- Davis, S. P., Abrams, M. C., Phillips, J. G., & Rao, M. L. P. 1988a, *JOSAB*, **5**, 2280
- Davis, S. P., Abrams, M. C., Sandalphon, Brault, J. W., & Rao, M. L. P. 1988b, *JOSAB*, **5**, 1838
- Davis, S. P., Phillips, J. G., Rao, M. L. P., & Abrams, M. C. 1988c, *JOSAB*, **5**, 2280
- Deslandres, H., & d'Azambuja, L. 1905, *Comptes Rendus*, **140**, 917
- Douay, M., Nietmann, R., & Bernath, P. F. 1988a, *JMoSp*, **131**, 250
- Douay, M., Nietmann, R., & Bernath, P. F. 1988b, *JMoSp*, **131**, 261
- Duxbury, G., Stamp, M. F., & Summers, H. P. 1998, *PPCF*, **40**, 361
- Erman, P., Larsson, M., Mannfors, B., & Lambert, D. L. 1982, *ApJ*, **253**, 983
- Fábri, C., Mátýus, E., Furtenbacher, T., et al. 2011, *JChPh*, **135**, 094307
- Fougere, P. F., & Nesbet, R. K. 1966, *JChPh*, **44**, 285
- Fox, J. G., & Herzberg, G. 1937, *PhRv*, **52**, 638
- Freymark, H. 1951, *AnP*, **8**, 221
- Furtenbacher, T., & Császár, A. G. 2012a, *JQSRT*, **113**, 929
- Furtenbacher, T., & Császár, A. G. 2012b, *JMoSt*, **1009**, 123
- Furtenbacher, T., Császár, A. G., & Tennyson, J. 2007, *JMoSp*, **245**, 115
- Furtenbacher, T., Szidarovszky, T., Fábri, C., & Császár, A. G. 2013a, *PCCP*, **15**, 10181
- Furtenbacher, T., Szidarovszky, T., Mátýus, E., Fábri, C., & Császár, A. G. 2013b, *J. Chem. Theory Comput.*, **9**, 5471
- Goebel, J. H., Bregman, J. D., Cooper, D. M., et al. 1983, *ApJ*, **270**, 190
- Goldman, A., & Cheskis, S. 2008, *ApPhB*, **92**, 281
- Goodwin, P. M., & Cool, T. A. 1988a, *JChPh*, **88**, 4548 (Erratum: Goodwin, P. M., 1989, *JChPh* **90**, 1296)
- Goodwin, P. M., & Cool, T. A. 1988b, *JChPh*, **89**, 6600
- Goodwin, P. M., & Cool, T. A. 1989, *JMoSp*, **133**, 230
- Goorvitch, D. 1990, *ApJS*, **74**, 769
- Gredel, R., Black, J. H., & Yan, M. 2001, *A&A*, **375**, 553
- Gredel, R., van Dishoeck, E. F., & Black, J. H. 1989, *ApJ*, **338**, 1047
- Gurvich, L., & Veyts, I. 1990, *Thermodynamic Properties Of Individual Substances: Elements and Compounds, Thermodynamic Properties of Individual Substances Series* (London: Taylor and Francis)
- Hall, P. B., & Maxwell, A. J. 2008, *ApJ*, **678**, 1292
- Hardwick, J. L., & Winicur, D. H. 1986, *JMoSp*, **115**, 175
- Herzberg, G. 1946, *PhRv*, **70**, 762
- Herzberg, G., Lagerqvist, A., & Malmberg, C. 1969, *CaJPh*, **47**, 2735
- Herzberg, G., & Sutton, R. B. 1940, *Can. J. Res.*, **18a**, 74
- Hobbs, L. M. 1979, *ApJL*, **232**, L175
- Hornbeck, G. A., & Herman, R. C. 1949, *JChPh*, **17**, 842
- Hornkohl, J. O., Nemes, L., & Parigger, C. 2011, in *Spectroscopy, Dynamics and Molecular Theory of Carbon Plasmas and Vapors*, ed. L. Nemes, & S. Irlé (Singapore: World Scientific), 139
- Huber, K. P., & Herzberg, G. 1979, *Molecular Spectra and Molecular Structure IV. Constants of Diatomic Molecules* (New York: Van Nostrand Reinhold Company)
- Hupe, R. C., Sheffer, Y., & Federman, S. R. 2012, *ApJ*, **761**, 38
- Iglesias-Groth, S. 2011, *MNRAS*, **411**, 1857
- Irwin, A. W. 1981, *ApJS*, **45**, 621
- Jackson, W. M., Bao, Y., & Urdahl, R. S. 1991, *JGR*, **96**, 17569
- Jiang, W., & Wilson, A. K. 2011, *JChPh*, **134**, 034101
- Joester, J. A., Nakajima, M., Reilly, N. J., et al. 2007, *JChPh*, **127**, 214303
- Kaminski, C. F., Hughes, I. G., & Ewart, P. 1997, *JChPh*, **106**, 5324
- Kaniki, J., Yang, X. H., Guo, Y. C., et al. 2003, *PNSci*, **13**, 736
- Kirby, K., & Liu, B. 1979, *JChPh*, **70**, 893

- Kokkin, D. L., Bacskay, G. B., & Schmidt, T. W. 2007, *JChPh*, **126**, 084302
- Kokkin, D. L., Reilly, N. J., Morris, C. W., et al. 2006, *JChPh*, **125**, 231101
- Kowalski, P. M. 2010, *A&A*, **519**, L8
- Krechivska, O., Bacskay, G. B., Troy, T. P., et al. 2015, *JPCA*, **119**, 12102
- Krechivska, O., Bacskay, G. B., Welsh, B. A., et al. 2016, *JChPh*, **144**, 144305
- Lambert, D. L. 1978, *MNRAS*, **182**, 249
- Lambert, D. L., Sheffer, Y., Danks, A. C., Arpigny, C., & Magain, P. 1990, *ApJ*, **353**, 640
- Lambert, D. L., Sheffer, Y., & Federman, S. R. 1995, *ApJ*, **438**, 740
- Landsverk, O. G. 1939, *PhRv*, **56**, 769
- Lebourlot, J., & Roueff, E. 1986, *JMoSp*, **120**, 157
- Lefebvre-Brion, H., & Field, R. W. 2004, *The Spectra and Dynamics of Diatomic Molecules* (Amsterdam: Elsevier)
- Lien, D. J. 1984, *ApJL*, **287**, L95
- Little, C. E., & Browne, P. G. 1987, *CPL*, **134**, 560
- Lloyd, G. M., & Ewart, P. 1999, *JChPh*, **110**, 385
- Martin, M. 1992, *J. Photochem. Photobio. A: Chem.*, **66**, 263
- Mayer, P., & O'Dell, C. R. 1968, *ApJ*, **153**, 951
- Meinel, H., & Messerle, G. 1968, *ApJ*, **154**, 381
- Messerle, G., & Krauss, L. 1967, *ZNatA*, **A 22**, 2015
- Müller, T., Dallos, M., Lischka, H., Dubrovay, Z., & Szalay, P. G. 2001, *Theor. Chem. Acc.*, **105**, 227
- Mulliken, R. S. 1939, *PhRv*, **56**, 778
- Nakajima, M., & Endo, Y. 2013, *JChPh*, **139**, 244310
- Nakajima, M., & Endo, Y. 2014, *JMoSp*, **302**, 9
- Nakajima, M., Joester, J. A., Page, N. I., et al. 2009, *JChPh*, **131**, 044301
- Petrova, T., & Sinitsa, L. 2006, *OptSp*, **101**, 871
- Phillips, J. G. 1948a, *ApJ*, **107**, 387
- Phillips, J. G. 1948b, *ApJ*, **110**, 73
- Phillips, J. G. 1968, *JMoSp*, **28**, 233
- Phillips, J. G., & Davis, S. P. 1968, *The Swan System of the C₂ Molecule* (Berkeley and Los Angeles: Univ. California)
- Pouilly, B., Robbe, J. M., Schamps, J., & Roueff, E. 1983, *JPhB*, **16**, 437
- Prasad, C. V. V., & Bernath, P. F. 1994, *ApJ*, **426**, 812
- Raffety, C. W. 1916, *PMag*, **32**, 546
- Rao, N. K., & Lambert, D. L. 2008, *MNRAS*, **384**, 477
- Rossi, S. C. F., Maciel, W. J., & Benevides-Soares, P. 1985, *A&A*, **148**, 93
- Rousselot, P., Laffont, C., Moreels, G., & Clairemidi, J. 1998, *A&A*, **335**, 765
- Rousselot, R., Hill, S. M., Burger, M. H., et al. 2000, *Icar*, **146**, 263
- Roux, F., Wannous, G., Michaud, F., & Verges, J. 1985, *JMoSp*, **109**, 334
- Sauval, A. J., & Tatum, J. B. 1984, *ApJS*, **56**, 193
- Schmidt, T. W., & Bacskay, G. B. 2011, *JChPh*, **134**, 224311
- Sherrill, C., & Piecuch, P. 2005a, *JChPh*, **122**, 124104
- Sherrill, C. D., & Piecuch, P. 2005b, *JChPh*, **122**, 124104
- Smith, G. P., Park, C., Schneiderman, J., & Luque, J. 2005, *CoFI*, **141**, 66
- Sonnentrucker, P., Welty, D. E., Thorburn, J. A., & York, D. G. 2007, *ApJS*, **168**, 58
- Sorkhabi, O., Blunt, V. M., Lin, H., et al. 1997, *JChPh*, **107**, 9842
- Souza, S. P., & Lutz, B. L. 1977, *ApJL*, **216**, L49
- Su, P., Wu, J., Gu, J., et al. 2011, *J. Chem. Theory Comput.*, **7**, 121
- Suzuki, T., Saito, S., & Hirota, E. 1985, *JMoSp*, **113**, 399
- Swan, W. 1857, *RSET*, **21**, 411
- Swings, P. 1943, *MNRAS*, **103**, 86
- Szidarovszky, T., & Császár, A. G. 2015, *JChPh*, **142**, 014103
- Tanabashi, A., & Amano, T. 2002, *JMoSp*, **215**, 285
- Tanabashi, A., Hirao, T., Amano, T., & Bernath, P. F. 2007, *ApJS*, **169**, 472 (Erratum: 2007 ApJS 170 261)
- Tennyson, J., Bernath, P. F., Brown, L. R., et al. 2009, *JQSRT*, **110**, 573
- Tennyson, J., Bernath, P. F., Brown, L. R., et al. 2010, *JQSRT*, **111**, 2160
- Tennyson, J., Bernath, P. F., Brown, L. R., et al. 2013, *JQSRT*, **117**, 29
- Tennyson, J., Bernath, P. F., Brown, L. R., et al. 2014a, *Pure Appl. Chem.*, **86**, 71
- Tennyson, J., Bernath, P. F., Brown, L. R., et al. 2014b, *JQSRT*, **142**, 93
- Tennyson, J., & Yurchenko, S. N. 2012, *MNRAS*, **425**, 21
- Urdahl, R. S., Bao, Y., & Jackson, W. M. 1988, *CPL*, **152**, 485
- van de Burgt, L. J., & Heaven, M. C. 1987, *JChPh*, **87**, 4235
- Van Orden, A., & Saykally, R. 1998, *ChRv*, **98**, 2313
- Vartya, M. S. 1970, *ARA&A*, **8**, 87
- Veseth, L. 1975, *CaJPh*, **53**, 299
- Vidler, M., & Tennyson, J. 2000, *JChPh*, **113**, 9766
- Watts, J. D., & Bartlett, R. J. 1992, *JChPh*, **96**, 6073
- Wehres, N., Romanzin, C., Linnartz, H., Van Winckel, H., & Tielens, A. G. G. M. 2010, *A&A*, **518**, A36
- Weltner, W., & Van Zee, R. J. 1989, *ChRv*, **89**, 1713
- Whiting, E. E. 1973, *Computer Program for Determining Rotational Line Intensity Factors for Diatomic Molecules* (Washington, DC: National Aeronautics and Space Administration)
- Wodtke, A. M., & Lee, Y. T. 1985, *JPhCh*, **89**, 4744
- Wollaston, W. H. 1802, *RSPTA*, **92**, 365
- Yan, W.-B., Curl, R., Merer, A. J., & Carrick, P. G. 1985, *JMoSp*, **112**, 436
- Yeung, S.-H., Chan, M.-C., Wang, N., & Cheung, A. S.-C. 2013, *CPL*, **557**, 31
- Yurchenko, S. N., Lodi, L., Tennyson, J., & Stolyarov, A. V. 2016a, *CoPhC*, **202**, 262
- Yurchenko, S. N., Tennyson, J., et al. 2016b, *MNRAS*, submitted